Available online at www.sciencedirect.com
ScienceDirect
Journal of Power Sources 164 (2007) 862–867
JOURNAL OF POWER SOURCES
www.elsevier.com/locate/jpowsour

Short communication

Electrochemical characterization of thermally oxidized natural graphite anodes in lithium-ion batteries

Joongpyo Shim [a,*], Kathryn A. Striebel [b]

[a] *Kunsan National University, School of Material Science & Chemical Engineering, Kunsan, Chonbuk 573-701, Korea*
[b] *Lawrence Berkeley National Laboratory, Environmental Energy Technologies Division, Berkeley, CA 94720, USA*

Received 26 June 2006; accepted 21 September 2006
Available online 4 December 2006

Abstract

Natural graphite, which is used as an anode material in lithium-ion batteries, is thermally treated to improve its cycleability and reduce irreversible reactions with the electrolyte. Natural graphite is treated in air at 550 °C. The weight loss increases when the thermal oxidation time is increased. The BET surface area of the graphite decreases with increasing weight loss. The cycleability and efficiency of the thermally oxidized natural graphite improves significantly. Thermal oxidation decreases the irreversible capacity for side-reactions with the electrolyte on the first cycle. By contrast, it does not change the reversible capacity and rate capability. The improvement in the cycleability after thermal oxidation may be due to the removal of imperfect sites on the graphite.
© 2006 Elsevier B.V. All rights reserved.

Keywords: Natural graphite; Anode; Thermal oxidation; Lithium-ion battery; Cycleability; Irreversible capacity

1. Introduction

Graphite, which is an excellent lithium intercalation compound, is widely used as the active material for the negative electrode (anode) in commercial rechargeable lithium batteries. Many types of graphite have been studied electrochemically to characterize their reversible capacity and first cycle irreversible capacity loss (ICL) due to the formation of a passivating solid electrolyte interface (SEI) layer. The dependence of performance on the particle size [1], surface area [2], surface modification [3] and mechanical milling [4] in various organic electrolytes has been cited, as well as these dependence of these parameters on the electrolyte composition [5].

The use of synthetic graphite in rechargeable lithium batteries for electric vehicles (EVs) or hybrid electric vehicles (HEVs) is prohibitive because of the relatively high costs. From this point of view, natural graphite (NG) would be a strong candidate for the replacement of synthetic graphite as an anode material because of its wide availability. The grinding and purification of raw natural graphite are critical processes in obtaining useful materials. Purification by heat treatments or chemical treatments in a strong acid can decrease the impurities in natural graphite [6]. Grinding, such as jet milling was found to be a more effective process to improve the reversible capacity of natural graphite [7,8]. A decrease of the particle size, however, increased the irreversible capacity loss at the first cycle because of the increase of contact area between electrolyte and graphite [1].

The electrochemical characteristics of mildly oxidized graphite have been reported by several groups. Peled et al. [9] reported that the mild oxidation of graphite in air induced acidic groups on the particle surface and that these groups formed a chemically-bonded SEI layer. They claimed that this stable layer was responsible for improved cycleability. Wu et al. [10] found that the irreversible capacity was decreased and the cycle performance was improved as a result of the elimination of some structural imperfections, such as edge carbon atoms and the introduction of nanochannels and micropores through oxidation. Rubino and Takeuchi [11] observed that the air oxidation of synthetic graphite increased the irreversible capacity through an increase in the surface area. On the other hand, there are several contrary phenomena reported in the literature. We present a detailed electrochemical characterization and a schematic mechanism for air-oxidized natural graphite.

* Corresponding author. Tel.: +82 63 469 4778; fax: +82 63 469 4778.
E-mail address: jpshim@kunsan.ac.kr (J. Shim).

0378-7753/$ – see front matter © 2006 Elsevier B.V. All rights reserved.
doi:10.1016/j.jpowsour.2006.09.111

2. Experimental

Natural graphite powder was mildly oxidized at 550 °C in air. A thermal gravimetric analyzer (TGA) was used to measure the weight loss during heat treatment. The BET surface area for pristine and oxidized natural graphite powder was determined by the nitrogen absorption method. The anode consisted of 90% natural graphite (SL20, average particle size 22 μm, Superior Graphite Co.) and 10% PVdF binder (Kynar) on a copper foil current-collector. Swagelok half-cells were assembled with 1-cm^2 electrodes, a porous polypropylene separator (Celgard 2500), a lithium foil reference/counter electrode and an electrolyte (1 M $LiPF_6$/ethylene carbonate (EC)/diethylene carbonate (DEC), LP40 from EM Industry). All cells were assembled for testing in an Ar-filled glove-box. Charge–discharge cycling was conducted for electrochemical characterization of the natural graphite anode. The anodes were cycled by an Arbin battery cycler between 0.01 and 1.0 V (versus Li/Li^+).

3. Results and discussion

3.1. Mild oxidation in air

Thermal gravimetric analysis (TGA) for the weight loss of natural graphite with respect to heating time at 550 °C in air is shown in Fig. 1. The weight loss increases linearly with respect to increasing heating time. Jiang et al. [12] have reported that the thermal oxidation of natural graphite in air increases the fraction of edge sites and decreases the fraction of basal plane sites as the particle size is decreased. The BET surface area of oxidized natural graphite with respect to weight loss is given in Fig. 2. Mild oxidation in air decreases the surface area of the natural graphite. The change in the surface area in graphite with oxidation depends on the crystal structure, impurities and surface morphology [13,14]. The pore-area distributions of pristine and oxidized graphites are presented in Fig. 3. Oxidized graphites have a very similar pore-area distribution compared with pristine graphite. Thermal treatment decreases the pore area significantly between pore diameters of 40 and 400 Å. In general, the thermal oxidation of carbon in air increases surface area, decreases particle size, and opens and enlarges the pores [15,16]. No explanation can be found for observed decrease in the surface area of our sample.

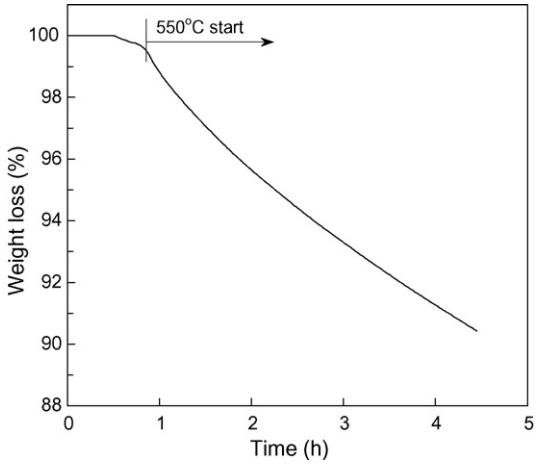

Fig. 1. Thermal gravimetric analysis (TGA) of natural graphite in air; scan rate 10 °C per min.

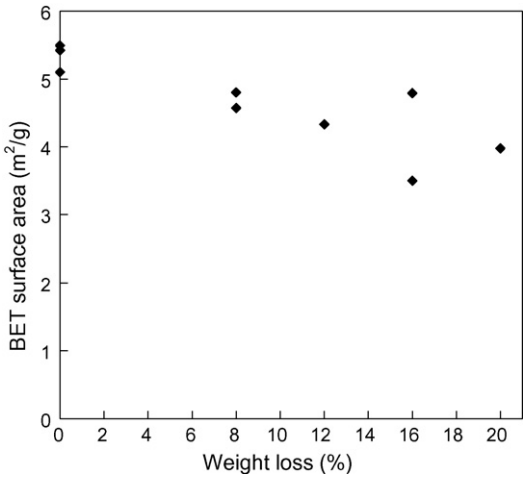

Fig. 2. Change in BET surface area of thermally oxidized natural graphite with weight loss.

3.2. Cycleability

The cycle performance, rate of capacity fade and average coulombic efficiency of the surface-oxidized natural graphite during constant C/2 cycling are shown in Figs. 4–6, respectively. The capacities of all samples are higher than the theoretical capacity of graphite (372 mAh g^{-1}) due to the increased capability to accommodate lithium ions in the cavities or micropores. The rate of capacity fade of the natural graphite anode decreases with respect to increased weight loss, and then remains unchanged after 12% weight loss. The improvement in coulombic efficiency, as seen in Fig. 6, is strongly related to the decrease in the rate of capacity fade. The surface oxidation of natural graphite in air clearly improves the cycle performance and increases the reversibility of the graphite particles.

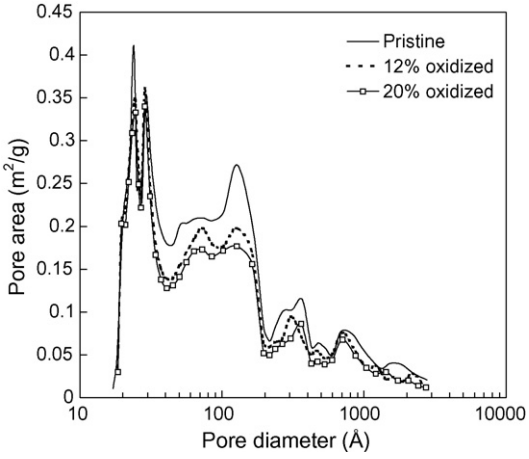

Fig. 3. Pore-area distribution of pristine and oxidized natural graphites.

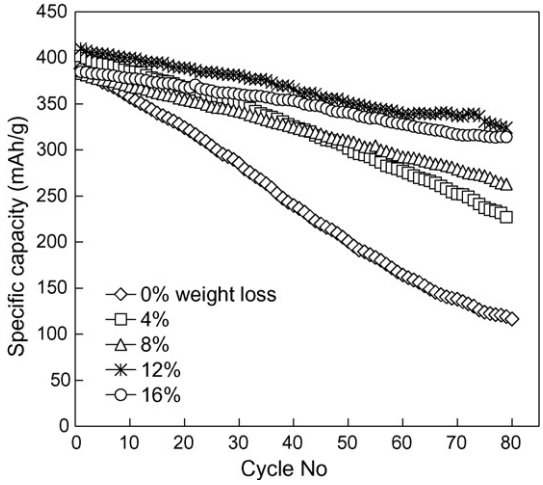

Fig. 4. Cycleability of pristine and oxidized natural graphite anodes at C/2; cut-off 0.01–1.0 V (vs. Li/Li$^+$).

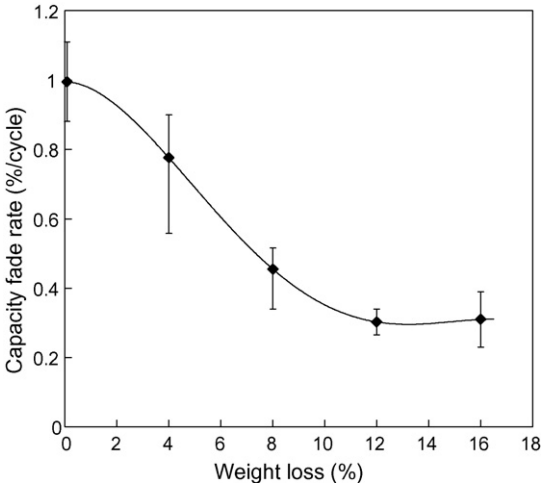

Fig. 5. Rate of capacity fade of pristine and oxidized natural graphite anodes during constant cycling.

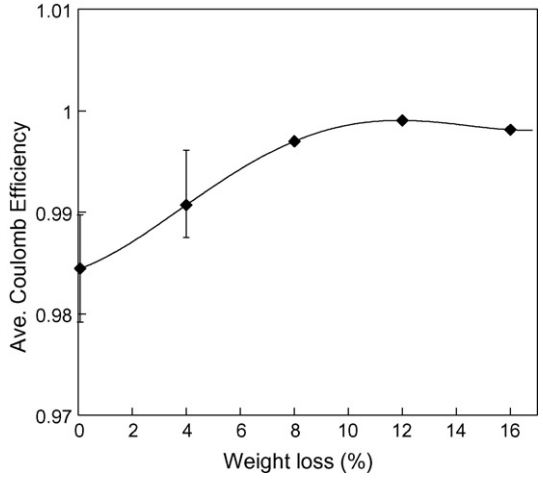

Fig. 6. Average coulombic efficiency for charge and discharge during constant cycling.

Table 1
Possible mechanisms and observed results for oxidized natural graphite

Possible change of graphite by oxidation	Changes to be expected	Results observed
Formation of an acidic group or an oxide layer on surface [18]	Side-reaction ↑ Thicker (or stable) SEI layer Irreversible capacity on first cycle ↑	No change in of total irreversible capacity. Irreversible capacity (side-reaction) ↓ Solvent decomposition ↓
Removal of structurally imperfect sites or impurities (organic or inorganic) [10]	Side-reaction ↓ Irreversible capacity on first cycle ↓	Efficiency during cycling ↑ Irreversible capacity (side-reaction) ↓
Introduction of microchannels (or micropores) or pore enlargement [9]	Lithium accommodation ↑ Lithium diffusion coefficient ↑ Capacity (reversible and irreversible) ↑ Rate capability ↑	BET surface area ↓ No change in reversible capacity. No change in rate capability

3.3. Possible mechanism for improvement of cycleability of oxidized graphite

The possible mechanisms and observed results regarding the changes in natural graphite after oxidation are summarized in Table 1. According to the proposal of Peled et al. [9], the acidic or oxide layer formed on the particle surface produces a stable SEI layer on the first cycle, which prevents further side-reactions with the electrolyte during cycling. More acidic (or oxide) layers would produce more side-reactions and increase the irreversible capacity on the first cycle. The removal of structurally imperfect sites or impurities, which was proposed by Wu et al. [10], could decrease the irreversible side-reactions involving the electrolyte. If an imperfect site or impurity could be removed through mild oxidation in air, the irreversible capacity would decrease and the efficiency on the first cycle or during cycling would increase. Nevertheless, we do not believe that an inorganic impurity, such as Fe, Cr, or Al can be eliminated by heat treatment at temperatures below 1000 °C. The formation of micropores [10] or the enlargement of the pores [17] would increase the surface area of the graphite. Several authors have observed a linear relationship with respect to irreversible capacity and surface area [1]. When the surface area of the graphite increases, the irreversible capacity during the first cycle also increases.

The voltage profiles of pristine and 16% oxidized natural graphite for the first cycle are shown in Fig. 7. The charge and discharge capacities and voltage profiles for both electrodes are very similar. The pristine sample exhibits a small plateau at around 0.75 V during lithium intercalation while the 16% oxidized natural graphite does not show a clear plateau at the same voltage. Fig. 8 shows dQ/dV plots for the pristine and oxidized natural graphites on the first cycle in the region of the formation of the SEI layer. Pristine natural graphite clearly shows two peaks at around 1.2 and 0.75 V. The small peak at 1.2 V almost disappears and the large peak at 0.75 V decreases significantly when the weight loss of the graphite increases as a result of

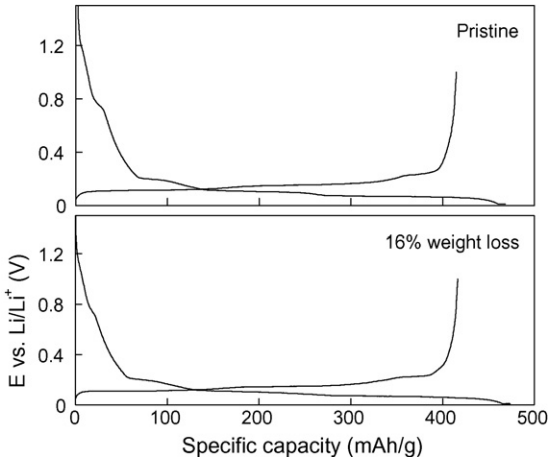

Fig. 7. Voltage profiles of pristine and 16% oxidized natural graphite on first cycle.

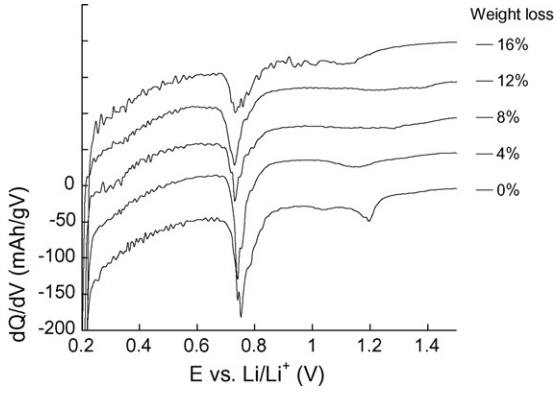

Fig. 8. dQ/dV plots of pristine and oxidized natural graphite anodes converted from Fig. 7.

heat treatment. The variation of irreversible capacity with thermal oxidation of natural graphite is presented in Fig. 9. The total irreversible capacity, which was calculated from the difference between the charge and discharge capacities, changes very little until a 12% weight loss, and then increased slightly at

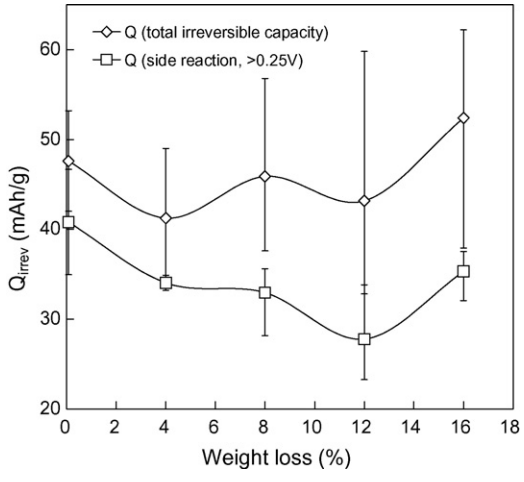

Fig. 9. Irreversible capacities for total and side-reaction above 0.25 V on first cycle.

16% weight loss. The irreversible capacity above 0.25 V (versus Li/Li$^+$), which is assigned to a side-reaction of the electrolyte, decreases until a 12% weight loss and then increases slightly. The irreversible capacities of the oxidized graphites due to side-reactions are still lower than those of the pristine graphite.

Several studies have reported the measured oxygen content on a graphite surface after thermal oxidation. Rubino and Takeuchi [11] found that the oxygen content was unchanged and the hydrogen content decreased for a 16%-burned off graphite [11]. Wu et al. [10] observed that the oxygen content decreased in a 9.33% oxidized sample [10]. Menachem et al. [18] determined changes in surface groups by XPS. They found that the oxygen content dropped to 2.5% for a 4.3% oxidized sample, remained constant for a 22% oxidized sample, and increases to 17% for a 34% oxidized sample [18]. They also observed that the irreversible capacity on the first cycle decreased continuously with respect to increasing weight loss of the graphite regardless of the oxygen content of the graphite. The irreversible capacity on the first cycle was linear with respect to the surface area of the graphite as reported by Zaghib et al. [1]. The decrease in irreversible capacity and surface area in Figs. 2 and 9 are very consistent until a 12% weight loss. We are, however, unable to explain why the irreversible capacity of the 16% oxidized sample increased again.

It is well known that the chemical reactivity at the basal plane sites is considerably lower than that at the edge or defect sites of carbon. For single-crystalline graphite, the oxidation rate of the carbon atoms at the edge sites below 800 °C is about 20 times greater than that at the basal plane surfaces [19]. The data in Fig. 3 shows that the pore distribution changes greatly between 40 and 400 Å. This indicates that the pores within this region predominantly react with oxygen and some of these pores are blocked or disappear. This change in the physical properties leads to a decrease in the irreversible reactions on the surface of the graphite, as shown in Figs. 5 and 9. The improvement in cycleability is mainly due to an increase in reversibility by thermal treatment of graphite, as demonstrated in Fig. 6. Thermal treatment in air may remove some structurally imperfect sites of graphite, which are involved in the irreversible reaction. The formation or growth of a thicker SEI layer, which is formed by a side-reaction on the initial cycle or during continuous cycling, may prevent further lithium intercalation. Thus, thermal treatment is considered to decrease the SEI layer.

Peled et al. [9] found that thermal treatment produced microchannels in the graphite and thereby increased lithium accommodation. Other workers observed [20] that air oxidation of graphite enlarged the pore diameter. The results given in Fig. 3 do not, however, show the introduction of any microchannels or enlargement of the pore diameters. In addition, no increase in the accommodation of lithium is detected after the thermal treatment, as shown in Fig. 10. To measure changes in lithium diffusion, measurements of the rate capability at 5 °C and the impedance as function of the state-of-charge (SOC) were collected. The results for pristine and oxidized graphite anodes are given in Figs. 11 and 12, respectively. The oxidized graphite anodes do not show any improvements in the rate capability compared with pristine graphite. This indicates that the elec-

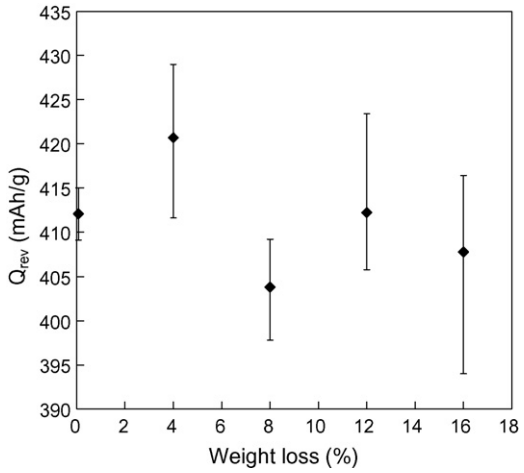

Fig. 10. Reversible capacities of pristine and oxidized natural graphite anodes on first cycle.

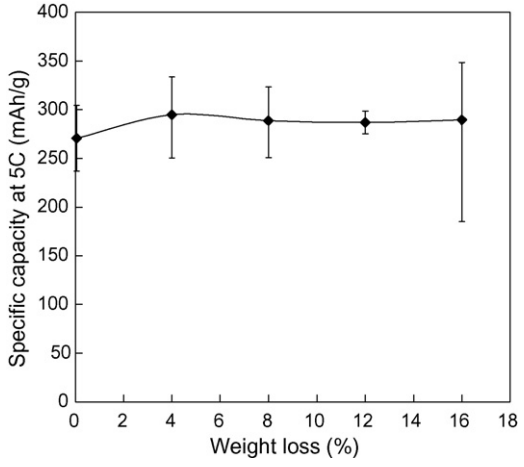

Fig. 11. Specific capacities of pristine and oxidized natural graphites at 5 °C.

trical conductivity of the oxidized graphite is unchanged. The lithium diffusion coefficient decreases slightly as the weight loss of the graphite by thermal treatment increases, as shown in Fig. 12. The average pore diameter measured by BJH adsorption decreased from 163 Å (pristine) to 147 Å (12% oxidized).

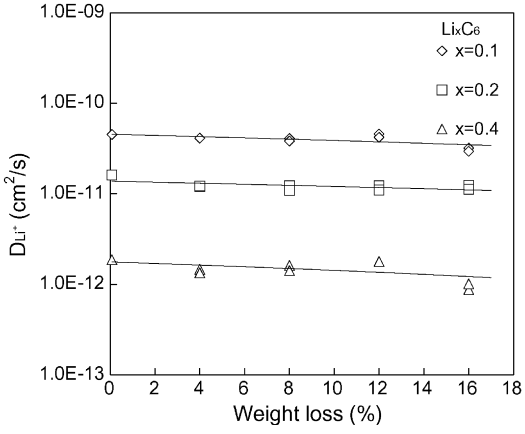

Fig. 12. Lithium diffusion coefficients of pristine and oxidized graphite anodes as function of state-of-charge.

This change in pore diameter may slightly decrease lithium diffusion.

Among three possible mechanisms proposed in other studies, the removal of the imperfect sites, which was suggested by Wu et al. [10], is consistent with the results presented here. It is found that the pore areas between 40 and 400 Å decreases after thermal oxidation, as shown in Fig. 3. Mesopores (20–500 Å diameter, IUPAC definition) in the graphite are predominantly attacked by oxygen. By contrast, pores between 20 and 40 Å do not experience any change in pore area. Oxygen molecules can easily reach the micropores (<20 Å) and pores of 20–40 Å in diameter because the molecular size of oxygen is approximately 2–3 Å. A reasonable explanation for the stability of the pores below 40 Å during thermal oxidation could not be found. Nevertheless, it can be concluded that imperfect sites with a pore diameter of 40–400 Å, which are very active sites and cause irreversible reactions with lithium ions, are removed through the attack of oxygen atoms, and that this removal significantly improves the cycleability of natural graphite. Chemical and morphological analyses will be the subject of future work.

4. Conclusion

Natural graphite that is thermally oxidized in air at 550 °C is found to possess improved electrochemical properties. Thermal oxidation linearly increases the weight loss and decreases the BET surface area of the graphite. The area of pores with diameters between 40 and 400 Å decreases markedly after thermal oxidation. The cycleability of thermally oxidized natural graphite anodes increases significantly due to improved efficiency. This treatment decreases the irreversible capacity of graphite for side-reactions with the electrolyte on the first cycle. On the other hand, the reversible capacity and the rate capability of graphite are not changed. Among three possible mechanisms proposed by other workers, namely, (i) the formation of an acidic group or oxide layer on the surface, (ii) the removal of structurally imperfect sites and (iii) the introduction of microchannels (or micropores) or pore enlargement, mechanism (ii) is consistent with the results obtained in this study.

Acknowledgements

The authors gratefully acknowledge the supply of natural graphite from Superior Graphite Company. The work was supported by the Assistant Secretary for Energy Efficiency and Renewable Energy, Office of FreedomCAR and Vehicle Technologies of the U.S. Department of Energy under Contract No. DE-AC03-76SF00098.

References

[1] K. Zaghib, G. Nadeau, K. Kinoshita, J. Electrochem. Soc. 147 (2000) 2110.
[2] K. Zaghib, F. Brochu, A. Guerfi, K. Kinoshita, J. Power Sources 103 (2001) 140.
[3] H. Wang, M. Yoshio, J. Power Sources 93 (2001) 123.
[4] T.S. Ong, H. Yang, Carbon 38 (2000) 2077.
[5] M. Fujimoto, Y. Shoji, Y. Kida, R. Ohshita, T. Nohma, K. Nishio, J. Power Sources 72 (1998) 226.

[6] K. Zaghib, X. Song, A. Guerfi, R. Rioux, K. Kinoshita, J. Power Sources 119–121 (2003) 8.
[7] H. Wang, T. Ikeda, K. Fukuda, M. Yoshio, J. Power Sources 83 (1999) 141.
[8] B. Simon, S. Flandrois, K. Guerin, A. Fevrier-Bouvier, I. Teulat, P. Biensan, J. Power Sources 81/82 (1999) 312.
[9] E. Peled, C. Menachem, D. Bar-Tow, A. Melman, J. Electrochem. Soc. 143 (1996) L4.
[10] Y.P. Wu, C. Jiang, C. Wan, R. Holze, Solid State Ionics 156 (2003) 283.
[11] R.S. Rubino, E.S. Takeuchi, J. Power Sources 81–82 (1999) 373.
[12] W. Jiang, G. Nadeau, K. Zaghib, K. Kinoshita, Thermochim. Acta 351 (2000) 85.
[13] E. Breval, M. Klimkiewicz, D.K. Agrawal, F. Rusinko Jr., Carbon 40 (2002) 1017.
[14] K. Zaghib, X. Song, K. Kinoshita, Thermochim. Acta 371 (2001) 57.
[15] P.A. Thrower, J.C. Bognet, G.K. Mathew, Carbon 20 (1982) 457.
[16] A. Braun, M. Bartsch, B. Schnyder, R. Kotz, O. Haas, A. Wokaun, Carbon 40 (2002) 375.
[17] J.S. Xue, J.R. Dahn, J. Electrochem. Soc. 142 (1995) 3668.
[18] C. Menachem, E. Peled, L. Burstain, Y. Resenberg, J. Power Sources 68 (1997) 277.
[19] K. Kinoshita, Carbon, Electrochemical and Physicochemical Properties, Wiley-Interscience publication, New York, 1988, p. 174.
[20] X. Chu, L.D. Schmidt, Carbon 9 (1991) 1251.